

The emerging role of hyperpolarized ^{129}Xe MRI in pulmonary hypertension

Fawaz Alenezi, Anna Costelle, Seth Lee, Bastiaan Driehuys & Sudarshan Rajagopal

To cite this article: Fawaz Alenezi, Anna Costelle, Seth Lee, Bastiaan Driehuys & Sudarshan Rajagopal (2025) The emerging role of hyperpolarized ^{129}Xe MRI in pulmonary hypertension, Expert Review of Respiratory Medicine, 19:12, 1161-1165, DOI: [10.1080/17476348.2025.2529543](https://doi.org/10.1080/17476348.2025.2529543)

To link to this article: <https://doi.org/10.1080/17476348.2025.2529543>



Published online: 10 Jul 2025.



Submit your article to this journal [↗](#)



Article views: 794



View related articles [↗](#)



View Crossmark data [↗](#)

EDITORIAL



The emerging role of hyperpolarized ^{129}Xe MRI in pulmonary hypertension

Fawaz Alenezi^a, Anna Costelle^b, Seth Lee^b, Bastiaan Driehuys^{b,c} and Sudarshan Rajagopal^a

^aDivision of Cardiology, Department of Medicine, Duke University Medical Center, Durham, NC, USA; ^bMedical Physics Program, Duke University, Durham, NC, USA; ^cDepartment of Radiology, Duke University School of Medicine, Durham, NC, USA

ARTICLE HISTORY Received 14 May 2025; Accepted 1 July 2025

KEYWORDS Hyperpolarized gas; xenon MRI; response to therapy; pulmonary hypertension; pulmonary arterial hypertension; heart failure

1. Introduction

^{129}Xe gas-exchange magnetic resonance imaging/spectroscopy (^{129}Xe MRI/MRS) is an emerging functional lung imaging technology that provides spatial and quantitative metrics of pulmonary ventilation, interstitial membrane uptake, transfer to capillary red blood cells (RBCs) and hemodynamics. When used in concert, these ^{129}Xe MRI/MRS metrics can differentiate between patients with chronic obstructive pulmonary disease (COPD), idiopathic pulmonary fibrosis (IPF), pulmonary arterial hypertension (PAH), and post-capillary pulmonary hypertension (PH). Here, we provide an overview of its potential in the evaluation of patients with PH, where ^{129}Xe MRI could offer important insights into disease pathophysiology, diagnosis, therapeutic response, and progression.

2. Xenon MRI technical background

Hyperpolarized ^{129}Xe MRI is a multi-breath hold technique that images ventilation and pulmonary gas exchange in three dimensions [1]. A patient inhales a small bag of hyperpolarized ^{129}Xe generated by a hyperpolarizer, and a ^{129}Xe MRI scan is obtained during a single breathhold maneuver over 10–15 s that can provide information on ventilation and gas exchange imaging [2]. These protocols have now been standardized to allow multi-site trials with this technology [3]. Inhaled ^{129}Xe , like O_2 , freely diffuses from the airspaces (*air-space phase*), across the pulmonary interstitial barrier tissues (*membrane phase*), and into the pulmonary capillaries where it transiently binds to hemoglobin in RBCs (*RBC phase*) (Figure 1A). In each of these three compartments (*airspace, membrane, and RBCs*), ^{129}Xe exhibits distinct spectral peaks (Figure 1B) [4]. These spectral signals can also be encoded spatially, thus visualizing the inhaled gas distribution in each lung compartment. Representative maps are shown for a range of patients (Figure 1C). These are interpreted as a 3D estimate of DL_{CO} , discerning its relative contributions from accessible alveolar volume, as well as membrane and capillary blood volume conductances (how easily the ^{129}Xe MRI gas can pass into that compartment) [5]. Notably, the ^{129}Xe -estimated membrane conductance can differentiate both emphysematous airspace enlargement in COPD (lower uptake), as well as

thickening of the interstitial membrane in ILD (higher uptake). Most pulmonary disease states exhibit significant RBC transfer defects; these reflect reduced gas exchange efficiency and are hypothesized to result from lost capillary blood volume.

Furthermore, the signal from ^{129}Xe dissolved in RBCs exhibits cardiogenic oscillations arising from the microvasculature (Figure 1C) [6,7]. This oscillation is due to changing capillary blood volume between systole and diastole [8]. Such oscillations were found in early studies to differentiate the hemodynamics in pre- and post-capillary PH, where PAH patients exhibited markedly lower than normal amplitude oscillations compared to controls, while left heart failure patients exhibited higher than normal values [9]. In PH in the setting of COPD or ILD, ^{129}Xe MRI reveals large RBC defects, i.e. RBC signal that is lower than two standard deviations below the normal, which could be due to decreased perfusion or vascular loss [9]. The presence of RBC defects artificially increases the RBC oscillation amplitudes and must be corrected. Thus, in patients without PH, the corrected oscillations return close to the normal 10% value, whereas for Group 3 patients with PH-ILD or PH-COPD corrected oscillations fall below 10%, and for post-capillary PH they remain above 10% (Figure 1C) [8]. Thus, with two 10-s breath-holds ^{129}Xe MRI and spectroscopy yields quantitative maps of gas exchange and a global measure of microvascular perfusion.

3. ^{129}Xe MRI metrics

Changes in signal in different gas exchange compartments have been associated with different disease states and specific changes in pulmonary function (Table 1).

3.1. Airspace signal

^{129}Xe MRI ventilation images are particularly sensitive and precise compared to pulmonary function testing since the acquisition is 3-dimensional and analyzed with reference to the patient's own lung shape. ^{129}Xe MRI ventilation defect percentage (VDP) has been shown to be highly reproducible in asthma across multiple sites [15] and cystic fibrosis with both high same-day and 28-day reproducibility [16]. VDP is often significantly elevated in obstructive lung diseases such

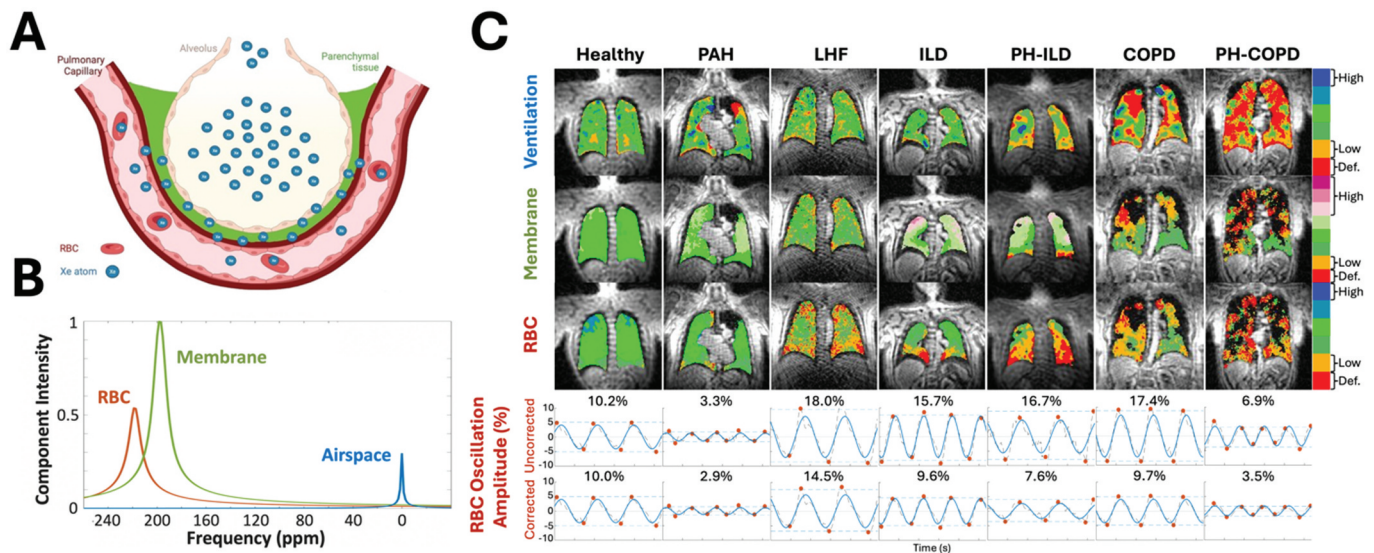


Figure 1. Hyperpolarized ^{129}Xe MRI/MRS. (a) ^{129}Xe diffuses from airspace into lung parenchymal tissue (membrane), and blood (RBCs). (b) ^{129}Xe has different MRI characteristics in airspace, membrane and RBCs. (c) (upper panel) ^{129}Xe MRI can be quantitatively compared to controls and areas of high and low signal visualized on a color scale. (lower panel) ^{129}Xe dissolved in RBCs exhibits cardiogenic oscillations. The amplitudes of these oscillations are increased in patients with RBC transfer defects. Correcting for RBC defects allows for the detection of PH and differentiation of left heart failure. def: defect. Panel (A) created in BioRender (<https://BioRender.com/oo9ocfj>).

Table 1. ^{129}Xe MRI/MRS metrics, their relationship to underlying pulmonary physiology, and their derangement in different disease states.

^{129}Xe MRI/MRS metrics	Region of Interest	Pulmonary Function	Derangements in Disease
^{129}Xe MRI ventilation defect percentage (VDP)	Ventilation (inhaled gas distribution)	Regional 3D quantification of ventilation heterogeneity and defects	Increased in obstructive lung disease [10,11].
^{129}Xe MRI membrane uptake percentage	Interstitial/membrane wall thickness and or loss of surface area	Regional 3D quantification of membrane thickening due to tissue, fibrosis and/or inflammation	Decreased in COPD [11] and increased in ILD [12].
^{129}Xe MRI RBC defect percentage	Alveolar-capillary interface gas exchange	Regional 3D quantification of gas exchange and indirect measure of capillary blood volume	Increased across a range of heart and lung diseases [9].
^{129}Xe MRS RBCs oscillation amplitude	Pulmonary capillary blood volume and hemodynamics	Quantification of capillary blood volume and hemodynamics	Abnormal in PAH and CTEPH [9,13].
^{129}Xe MRI RBCs defect/membrane uptake ratio	Gas exchange/interstitial wall thickness ratio	Regional 3D quantification of gas exchange to fibrosis and inflammation	Abnormal across a range of heart and lung diseases [9].
^{129}Xe MRI RBC chemical shift	Pulmonary microcirculation	Strongly depends on blood oxygenation	Abnormal across a range of diseases with hypoxia [14].

as asthma, COPD, and cystic fibrosis [10]. Conversely, a homogeneous ventilation pattern with low VDP supports the absence of significant airway obstruction, as is observed in healthy individuals, or those with restrictive lung diseases or PH [9].

3.2. Membrane signal

In gas exchange, the membrane tissues serve as a diffusive barrier for gas transfer to the RBCs. Their integrity can be characterized by imaging their ^{129}Xe uptake, which is often high (>2 standard deviations above normal) in interstitial lung diseases (ILDs) such as idiopathic pulmonary fibrosis (IPF) [17], nonspecific interstitial pneumonias (NSIP) [12] and chronic hypersensitivity pneumonitis (CHP) [18]. Conversely, membrane uptake is reduced in emphysema [19] (Figure 1 (c)), likely due to lung parenchymal destruction. Recent work suggested that COPD patients with normal membrane uptake, e.g. chronic bronchitis, were more likely to respond to bronchodilator treatments vs those with emphysema [12].

3.3. RBC transfer

Most cardiopulmonary diseases exhibit marked RBC transfer defects on gas exchange ^{129}Xe MRI, including ILD, PH, and COPD [9]. In Group 1 PH, decreased RBC transfer is often the primary abnormal finding on ^{129}Xe MRI, with relatively preserved airspace and membrane signals [9]. In patients with ILD, the RBC defect pattern commonly exhibits a distinct basal pattern [20]. However, the spatial patterns of RBC transfer, which reflect pulmonary vascular remodeling and vascular dropout, are not pathognomonic for these diseases.

3.4. Spectroscopic measures

While ^{129}Xe imaging receives attention for the regional information it provides, global spectroscopy can be used to understand whole-lung effects such as overall blood oxygenation [14,21] or microvascular function [7]. Hyperpolarized ^{129}Xe exhibits distinct chemical shifts as it dissolves in membrane tissue (197.6 ± 0.3 ppm) and is transferred to RBCs (218.2 ± 0.5 ppm). While the membrane shift is fixed, the RBC shift

depends strongly on blood oxygenation [14]. In patients with substantial RBC transfer defects (with a loss of capillary blood volume), RBC shifts are diminished [7,12]. Since they are measured within the capillary bed, they reflect the average oxygenation during the transit time; loss of capillaries decreases transit time and thus average RBC shift, even if O₂ saturation does eventually reach normal values.

Spectra acquired dynamically reveal a cardiogenically oscillating RBC signal amplitude [6,7]. These oscillations are now understood to be driven by the resistance of the pulmonary capillary and venous vasculature, changes in blood flow between systole and diastole, as well as the compliance of the pulmonary capillaries [8]. In patients with RBC defects, pulmonary capillary impedance increases, driving the oscillation amplitudes up. This requires correcting for RBC transfer defects, thereby improving the detection of PH. Recently, oscillation amplitudes, when corrected for reduced capillary blood volume, were shown to decrease significantly with elevated pulmonary vascular resistance (PVR) at right heart catheterization [8]. This work showed that whole-lung oscillations were indirectly sensitive to elevated pre-capillary resistance, directly sensitive to post-capillary impedance, and if they can be spatially resolved, the sensitivity to PH would be dramatically improved. However, one practical finding was that whole-lung corrected oscillations below 7.5% were 100% specific for elevated PVR [8].

3.5. Cardiogenic RBC oscillations

Direct sensitivity to PVR, as well as spatial information on the location or heterogeneity of vascular defects, can be obtained by imaging the RBC oscillations. Fortuitously, the RBC oscillations are embedded within the gas exchange images themselves. Thus, they can be mapped by reconstructing the portions of the image acquired during systole vs diastole and subtracting those images [22]. These spatially resolved

maps allow for direct visualization of reduced or elevated RBC oscillation amplitudes, providing higher sensitivity for the detection and characterization of PH than global oscillations alone. Such RBC oscillation images have been constructed in patients with chronic thromboembolic pulmonary hypertension (CTEPH), where capillary blood volume distal to the thrombus showed little to no oscillations [21]. These areas of oscillation defects corresponded to surgically confirmed segmental disease and were resolved following pulmonary endarterectomy. Notably, the gas exchange images themselves displayed no noticeable changes in RBC transfer, consistent with no change in capillary blood volume, while the cardiogenic oscillations represent actual flow (Figure 2). However, the accurate and robust recovery of oscillation maps is an area of active development.

4. Potential clinical applications of xenon MRI in PH

The diagnosis and follow-up of patients with PH is challenging due to the absence of clear biomarkers that reflect the complexity of its underlying pathophysiology. As discussed above, ¹²⁹Xe MRI/MRS provides important insights into pulmonary pathophysiology, including its derangements in PH. The current clinical diagnosis of PH often relies on population-based 'normal' values that do not account for patient-specific physiology related to age or coexisting heart and lung diseases. The unique properties of ¹²⁹Xe MRI offer potential solutions to this significant clinical need for noninvasive diagnostic testing in PH. In initial studies, ¹²⁹Xe MRI metrics displayed a unique profile in PAH compared to other common heart and lung diseases, including COPD, IPF, and left heart failure [9]. Specifically, patients with PAH displayed relatively normal airspace and membrane signals, but displayed decreased RBC signal [9]. Notably, these same findings were largely consistent with the pattern observed in a monocrotaline rat model of PH, where ¹²⁹Xe MRI displayed RBC defects, although with some

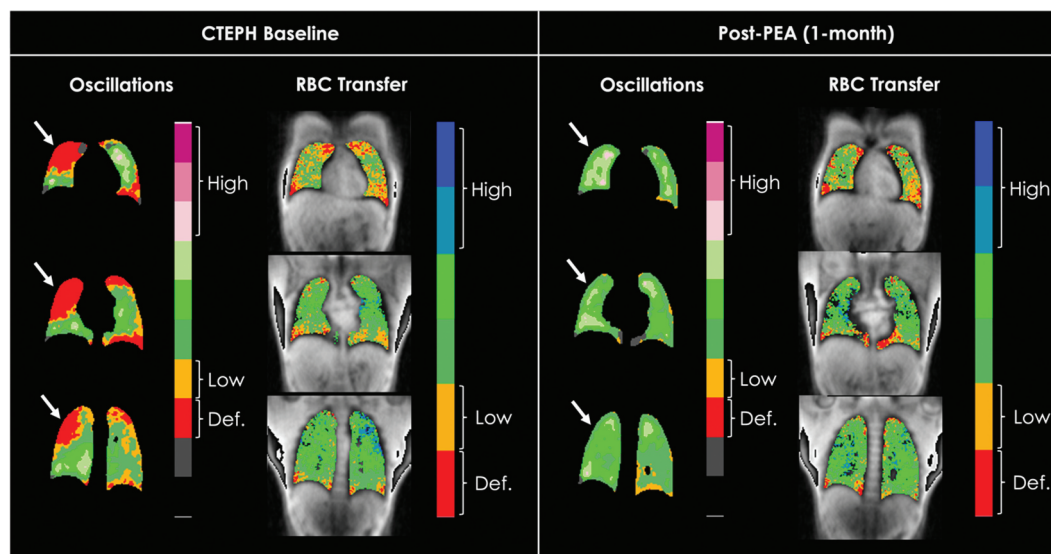


Figure 2. Imaging RBC transfer and RBC oscillation amplitudes in chronic thromboembolic pulmonary hypertension (CTEPH). Prior to pulmonary endarterectomy (PEA), RBC oscillation maps show significant defects (red) in the right upper and middle lobes. After PEA, these defects are eliminated suggesting flow has returned. However, RBC transfer maps reflecting the capillary blood volume look largely normal at baseline and remain largely unchanged after surgery.

airspace and membrane abnormalities likely due to the inflammation induced by monocrotaline in this disease model [23]. An initial diagnostic algorithm based on RBC abnormalities and decreased cardiogenic oscillations in the MRS signal displayed good accuracy in detecting PH [24]. More recently, correction of these RBC oscillation amplitudes by RBC defect percentage resulted in an improved model to estimate elevated PVR [8].

Recently, ^{129}Xe MRI metrics have also been shown to be sensitive to an acute response to therapy in PH patients treated with inhaled treprostinil [25], with statistically significant improvements observed in RBC transfer and the RBC/Membrane ratio. This 20% increase in mean RBC/Membrane ratio, consistent with an increase in capillary blood volume, was observed in a cohort of only 11 patients at 15 min. The ability to monitor an acute response to therapy suggests that ^{129}Xe MRI will be sensitive to the effects of PAH-targeted therapies over longer periods of time, and suggests that ^{129}Xe MRI could be a useful tool in assessing response to therapy and guiding management in PH.

5. Summary

^{129}Xe MRI provides noninvasive measurements of pulmonary ventilation, lung tissue microstructure, and transfer to red blood cells in the pulmonary capillaries, providing new opportunities to deeply investigate lung diseases. These studies suggest that ^{129}Xe MRI has the potential to add new insight by regionally visualizing functional changes and hemodynamics.

Abbreviations

CHP	Chronic hypersensitivity pneumonitis
COPD	Chronic obstructive pulmonary disease.
CTEPH	Chronic thromboembolic pulmonary hypertension
ILD	interstitial lung disease
IPF	Idiopathic pulmonary fibrosis
LHF	left heart failure
MRI	Magnetic resonance imaging
MRS	Magnetic resonance spectroscopy
NSIP	Non-specific interstitial pneumonias
PAH	Pulmonary arterial hypertension
PH	Pulmonary hypertension
PH-COPD	PH associated with COPD
PH-ILD	PH associated with ILD
PVR	Pulmonary vascular resistance
RBCs	Red blood cells
VDP	Ventilation defect percentage

Funding

F Alenezi is supported by an AHA Career Development Award. S Rajagopal is supported by [R01HL153872] and a Mandel Seed Award. B Driehuis is supported by [R01HL153872 and R01HL105643].

Declarations of interest

B Driehuis is the founder of and consultant to Polarean Imaging. The authors have no other relevant affiliations or financial involvement with any organization or entity with a financial interest in or financial conflict

with the subject matter or materials discussed in the manuscript apart from those disclosed.

Reviewer disclosures

Peer reviewers on this manuscript have no relevant financial or other relationships to disclose.

References

Papers of special note have been highlighted as either of interest (*) or of considerable interest () to readers.**

- Mugler JP, Altes TA. Hyperpolarized ^{129}Xe MRI of the human lung. *J Magn Reson Imaging*. 2013;37(2):313–331. doi: 10.1002/jmri.23844
- Niedbalski PJ, Willmering MM, Thomen RP, et al. A single-breath-hold protocol for hyperpolarized (^{129}Xe) ventilation and gas exchange imaging. *NMR Biomed*. 2023;36(8):e4923. doi: 10.1002/nbm.4923
- Niedbalski PJ, Hall CS, Castro M, et al. Protocols for multi-site trials using hyperpolarized (^{129}Xe) MRI for imaging of ventilation, alveolar-airspace size, and gas exchange: a position paper from the (^{129}Xe) MRI clinical trials consortium. *Magn Reson Med*. 2021;86(6):2966–2986. doi: 10.1002/mrm.28985
- This manuscript describes up-to-date protocols for obtaining Xe MRI.**
- Chen RY, Fan FC, Kim S, et al. Tissue-blood partition coefficient for xenon: temperature and hematocrit dependence. *J Appl Physiol Respir Environ Exerc Physiol*. 1980;49(2):178–183. doi: 10.1152/jap.1980.49.2.178
- Wang Z, Rankine L, Bier EA, et al. Using hyperpolarized (^{129}Xe) gas-exchange MRI to model the regional airspace, membrane, and capillary contributions to diffusing capacity. *J Appl Physiol*. (2021;130(5):1398–1409. doi: 10.1152/jap.2021.130.5.1398
- Norquay G, Leung G, Stewart NJ, et al. Relaxation and exchange dynamics of hyperpolarized ^{129}Xe in human blood. *Magn Reson Med*. 2015;74(2):303–311. doi:10.1002/mrm.25417
- Bier EA, Robertson SH, Schrank GM, et al. A protocol for quantifying cardiogenic oscillations in dynamic (^{129}Xe) gas exchange spectroscopy: the effects of idiopathic pulmonary fibrosis. *NMR Biomed*. 2019;32(1):e4029. doi: 10.1002/nbm.4029
- Costelle A, Lu J, Leewiwatwong S, et al. Combining hyperpolarized (^{129}Xe) MR imaging and spectroscopy to noninvasively estimate pulmonary vascular resistance. *J Appl Physiol*. (2025;138(3):623–633. doi: 10.1152/jap.2024.138.3.623
- This manuscript describes how Xe MR spectroscopy can be used to noninvasively estimate pulmonary vascular resistance.**
- Wang Z, Bier EA, Swaminathan A, et al. Diverse cardiopulmonary diseases are associated with distinct xenon magnetic resonance imaging signatures. *Eur Respir J*. 2019;54(6):1900831. doi: 10.1183/13993003.00831-2019
- ** This manuscript describes how Xe MRI patterns can differentiate different chronic heart and lung diseases.**
- Thomen RP, Walkup LL, Roach DJ, et al. Hyperpolarized ^{129}Xe for investigation of mild cystic fibrosis lung disease in pediatric patients. *J Cyst Fibros*. 2017;16(2):275–282. doi: 10.1016/j.jcf.2016.07.008
- Myc L, Qing K, He M, et al. Characterisation of gas exchange in COPD with dissolved-phase hyperpolarised xenon- ^{129}Xe MRI. *Thorax*. 2021;76(2):178–181. doi: 10.1136/thoraxjnl-2020-214924
- Mummy DG, Bier EA, Wang Z, et al. Hyperpolarized (^{129}Xe) MRI and Spectroscopy of gas-exchange abnormalities in nonspecific interstitial pneumonia. *Radiology*. 2021;301(1):211–220. doi: 10.1148/radiol.2021204149
- Lu J, Alenezi F, Bier E, et al. Optimized quantitative mapping of cardiopulmonary oscillations using hyperpolarized (^{129}Xe) gas exchange MRI: digital phantoms and clinical evaluation in

- CTEPH. *Magn Reson Med.* 2024;91(4):1541–1555. doi: [10.1002/mrm.29965](https://doi.org/10.1002/mrm.29965)
14. Norquay G, Leung G, Stewart NJ, et al. (129) Xe chemical shift in human blood and pulmonary blood oxygenation measurement in humans using hyperpolarized (129) Xe NMR. *Magn Reson Med.* 2017;77(4):1399–1408. doi: [10.1002/mrm.26225](https://doi.org/10.1002/mrm.26225)
 15. Svenningsen S, McIntosh M, Ouriadov A, et al. Reproducibility of hyperpolarized (129)Xe MRI ventilation defect percent in severe asthma to evaluate clinical trial feasibility. *Acad Radiol.* 2021;28(6):817–826. doi: [10.1016/j.acra.2020.04.025](https://doi.org/10.1016/j.acra.2020.04.025)
 16. Walkup LL, Roach DJ, Plummer JW, et al. Same-day repeatability and 28-day reproducibility of xenon MRI ventilation in children with cystic fibrosis in a multi-site trial. *J Magn Reson Imaging.* 2025;61(4):1664–1674. doi: [10.1002/jmri.29605](https://doi.org/10.1002/jmri.29605)
 17. Kaushik SS, Freeman MS, Yoon SW, et al. Measuring diffusion limitation with a perfusion-limited gas–hyperpolarized 129Xe gas-transfer spectroscopy in patients with idiopathic pulmonary fibrosis. *J Appl Physiol.* 1985 117(6):577–585. doi: [10.1152/jappphysiol.00326.2014](https://doi.org/10.1152/jappphysiol.00326.2014)
 18. Wulfeck MK, Mummy DG, Zhang S, et al. Hyperpolarized (129)Xe MRI and spectroscopy of gas exchange abnormalities in chronic hypersensitivity pneumonitis. *Respir Med.* 2024;234:107827. doi: [10.1016/j.rmed.2024.107827](https://doi.org/10.1016/j.rmed.2024.107827)
 19. Kirby M, Svenningsen S, Owrangi A, et al. Hyperpolarized 3He and 129Xe MR imaging in healthy volunteers and patients with chronic obstructive pulmonary disease. *Radiology.* 2012;265(2):600–610. doi: [10.1148/radiol.12120485](https://doi.org/10.1148/radiol.12120485)
 20. Wang JM, Robertson SH, Wang Z, et al. Using hyperpolarized (129)Xe MRI to quantify regional gas transfer in idiopathic pulmonary fibrosis. *Thorax.* 2018;73(1):21–28. doi: [10.1136/thoraxjnl-2017-210070](https://doi.org/10.1136/thoraxjnl-2017-210070)
 21. Wolber J, Cherubini A, Leach MO, et al. Hyperpolarized Xe-129 NMR as a probe for blood oxygenation. *Magn Reson Med.* 2000;43(4):491–496. doi: [10.1002/\(SICI\)1522-2594\(200004\)43:4<491::AID-MRM1>3.0.CO;2-6](https://doi.org/10.1002/(SICI)1522-2594(200004)43:4<491::AID-MRM1>3.0.CO;2-6)
 22. Niedbalski PJ, Bier EA, Wang Z, et al. Mapping cardiopulmonary dynamics within the microvasculature of the lungs using dissolved (129)Xe MRI. *J Appl Physiol.* (2020);129(2):218–229. doi: [10.1152/jappphysiol.00186.20201985](https://doi.org/10.1152/jappphysiol.00186.20201985)
 23. Virgincar RS, Nouls JC, Wang Z, et al. Quantitative (129)Xe MRI detects early impairment of gas-exchange in a rat model of pulmonary hypertension. *Sci Rep.* 2020;10(1):7385. doi: [10.1038/s41598-020-64361-1](https://doi.org/10.1038/s41598-020-64361-1)
 24. Bier EA, Alenezi F, Lu J, et al. Noninvasive diagnosis of pulmonary hypertension with hyperpolarised (129)Xe magnetic resonance imaging and spectroscopy. *ERJ Open Res.* 2022;8(2):00035–2022. doi: [10.1183/23120541.00035-2022](https://doi.org/10.1183/23120541.00035-2022)
 25. Alenezi F, Costelle A, Sharma P, et al. Xenon-129 magnetic resonance imaging and spectroscopy detects response to therapy in pulmonary hypertension. *Eur Respir J.* 2025;65(2):2401651. doi: [10.1183/13993003.01651-2024](https://doi.org/10.1183/13993003.01651-2024)
- **This manuscript demonstrates that Xe MRI RBC transfer is sensitive to the acute effect of inhaled treprostinil in patients with PAH.**